



Calhoun: The NPS Institutional Archive
DSpace Repository

Theses and Dissertations

1. Thesis and Dissertation Collection, all items

1997-12

Design, construction and testing of an autonomous mine hunter

Schmidt, Jeffrey A

Monterey, California. Naval Postgraduate School

<http://hdl.handle.net/10945/8216>

Downloaded from NPS Archive: Calhoun



<http://www.nps.edu/library>

Calhoun is the Naval Postgraduate School's public access digital repository for research materials and institutional publications created by the NPS community. Calhoun is named for Professor of Mathematics Guy K. Calhoun, NPS's first appointed -- and published -- scholarly author.

Dudley Knox Library / Naval Postgraduate School
411 Dyer Road / 1 University Circle
Monterey, California USA 93943

NPS ARCHIVE
1997.12
SCHMIDT, J.

NAVAL POSTGRADUATE SCHOOL MONTEREY, CALIFORNIA



THESIS

DESIGN, CONSTRUCTION AND TESTING OF AN
AUTONOMOUS MINE HUNTER

by

Jeffrey A. Schmidt

December, 1997

Thesis Advisor:
Thesis Advisor:

Richard Harkins
Xiaoping Yun

Thesis
S337222

Approved for public release; distribution is unlimited.

DUDLEY KNOX LIBRARY
NAVAL POSTGRADUATE SCHOOL
MONTEREY CA 93943-5101

**DUDLEY KNOX LIBRARY
NAVAL POSTGRADUATE SCHOOL
MONTEREY, CA 93943-5101**

REPORT DOCUMENTATION PAGE

Form Approved OMB No. 0704-0188

Public reporting burden for this collection of information is estimated to average 1 hour per response, including the time for reviewing instruction, searching existing data sources, gathering and maintaining the data needed, and completing and reviewing the collection of information. Send comments regarding this burden estimate or any other aspect of this collection of information, including suggestions for reducing this burden, to Washington Headquarters Services, Directorate for Information Operations and Reports, 1215 Jefferson Davis Highway, Suite 1204, Arlington, VA 22202-4302, and to the Office of Management and Budget, Paperwork Reduction Project (0704-0188) Washington DC 20503

1. AGENCY USE ONLY (Leave blank)	2. REPORT DATE December 1997.	3. REPORT TYPE AND DATES COVERED Master's Thesis	
4. TITLE OF THESIS. Design, Construction and Testing of an Autonomous Mine Hunter		5. FUNDING NUMBERS	
6. AUTHOR(S) Schmidt, Jeffrey, A.			
7. PERFORMING ORGANIZATION NAME(S) AND ADDRESS(ES) Naval Postgraduate School Monterey CA 93943-5000		8. PERFORMING ORGANIZATION REPORT NUMBER	
9. SPONSORING/MONITORING AGENCY NAME(S) AND ADDRESS(ES)		10. SPONSORING/MONITORING AGENCY REPORT NUMBER	
11. SUPPLEMENTARY NOTES The views expressed in this thesis are those of the author and do not reflect the official policy or position of the Department of Defense or the U.S. Government.			
12a. DISTRIBUTION/AVAILABILITY STATEMENT Approved for public release; distribution is unlimited.		12b. DISTRIBUTION CODE	
13. ABSTRACT (maximum 200 words) Landmine detection is a immense technological problem. A small, low power metal detector would find application in concert with other search technologies. A detection circuit was designed and constructed consisting of a search coil and a CMOS exclusive OR gate forming an oscillator. This was interfaced to a microprocessor which counted the pulses from the oscillator and decided whether a detection had been made. Detection range for an anti-personnel mine like object was 14 cm at the coil centerline. A robot platform to autonomously search for landmines was constructed..			
14. SUBJECT TERMS Landmine, Induction, Robot, Microprocessor.		15. NUMBER OF PAGES 56	
		16. PRICE CODE	
17. SECURITY CLASSIFICATION OF REPORT Unclassified	18. SECURITY CLASSIFICATION OF THIS PAGE Unclassified	19. SECURITY CLASSIFICATION OF ABSTRACT Unclassified	20. LIMITATION OF ABSTRACT UL

Approved for public release; distribution is unlimited.

**DESIGN, CONSTRUCTION AND TESTING
OF AN AUTONOMOUS MINE HUNTER**

Jeffrey A. Schmidt

Lieutenant, United States Navy

B.S., University of South Carolina, 1988

Submitted in partial fulfillment
of the requirements for the degree of

MASTER OF SCIENCE IN APPLIED PHYSICS

from the

NAVAL POSTGRADUATE SCHOOL

December 1997

Gregory A. Schmidt

NPS Archive
1997.12
Schmidt, J.

~~1 box~~
~~838/7222~~
~~C. 2~~

ABSTRACT

Landmine detection is a immense technological problem. A small, low power metal detector would find application in concert with other search technologies. A detection circuit was designed and constructed consisting of a search coil and a CMOS exclusive OR gate forming an oscillator. This was interfaced to a microprocessor which counted the pulses from the oscillator and decided whether a detection had been made. Detection range for an anti-personnel mine like object was 14 cm at the coil centerline. A robot platform to autonomously search for landmines was constructed.

TABLE OF CONTENTS

I. INTRODUCTION	1
II. THEORY	3
A. REVIEW OF SENSING TECHNOLOGIES	3
1. Electromagnetic	3
2. Miscellaneuos	6
B. COIL THEORY	7
1. Magnetic Field and Flux	7
2. Inductance	8
3. Mutual Induction	9
C. RLC OSCILLATOR THEORY	9
III. CONSTRUCTION AND OPERATION	13
A. SENSING CIRCUIT	13
B. SENSING COIL	15
C. OSCILLATOR CIRCUIT CONSTRUCTION	16
D. OSCILLATOR CIRCUIT OPERATION	17
E. COUNTING CIRCUIT	24
F. MICROPROCESSOR	24
G. SAMPLING CIRCUIT OPERATION	25
H. ROBOT	26
1. 68HC11	27
2. 68HC11 / Tiny Giant Interface	28
3. Pulse Width Modulation	28
4. Motor Drive Chip	29
5. Motors and Shaft Encoders	30
6. Wheel / Speed Control	30
IV. TEST RESULTS AND CONCLUSIONS	31
A. TEST RESULTS	31
B. FUTURE WORK	33
C. CONCLUSION	33
APPENDIX A. TINY GIANT C CODE	35
APPENDIX B. 68HC11 C CODE	37
LIST OF REFERENCES	43
INITIAL DISTRIBUTION LIST	45

ACKNOWLEDGEMENT

I would like to thank my advisors, Richard Harkins and Xiaoping Yun for the freedom to tie myself in knots, and then the patience to untie me. George Jaksha brought his mechanical genius to bear many times during this project, and was a reliable sounding board for my ideas. Warren Rogers went above and beyond the call in explaining the finer points of circuit analysis. Finally, thanks to my wife Jay and daughter Jessi, for without whom none of this would mean much.

TABLE I		TABLE II	
Year	Value	Year	Value
1950	100	1955	100
1951	105	1956	105
1952	110	1957	110
1953	115	1958	115
1954	120	1959	120
1960	125	1960	125
1961	130	1961	130
1962	135	1962	135
1963	140	1963	140
1964	145	1964	145
1965	150	1965	150
1966	155	1966	155
1967	160	1967	160
1968	165	1968	165
1969	170	1969	170
1970	175	1970	175
1971	180	1971	180
1972	185	1972	185
1973	190	1973	190
1974	195	1974	195
1975	200	1975	200
1976	205	1976	205
1977	210	1977	210
1978	215	1978	215
1979	220	1979	220
1980	225	1980	225
1981	230	1981	230
1982	235	1982	235
1983	240	1983	240
1984	245	1984	245
1985	250	1985	250
1986	255	1986	255
1987	260	1987	260
1988	265	1988	265
1989	270	1989	270
1990	275	1990	275
1991	280	1991	280
1992	285	1992	285
1993	290	1993	290
1994	295	1994	295
1995	300	1995	300
1996	305	1996	305
1997	310	1997	310
1998	315	1998	315
1999	320	1999	320
2000	325	2000	325
2001	330	2001	330
2002	335	2002	335
2003	340	2003	340
2004	345	2004	345
2005	350	2005	350
2006	355	2006	355
2007	360	2007	360
2008	365	2008	365
2009	370	2009	370
2010	375	2010	375
2011	380	2011	380
2012	385	2012	385
2013	390	2013	390
2014	395	2014	395
2015	400	2015	400
2016	405	2016	405
2017	410	2017	410
2018	415	2018	415
2019	420	2019	420
2020	425	2020	425
2021	430	2021	430
2022	435	2022	435
2023	440	2023	440
2024	445	2024	445
2025	450	2025	450
2026	455	2026	455
2027	460	2027	460
2028	465	2028	465
2029	470	2029	470
2030	475	2030	475
2031	480	2031	480
2032	485	2032	485
2033	490	2033	490
2034	495	2034	495
2035	500	2035	500
2036	505	2036	505
2037	510	2037	510
2038	515	2038	515
2039	520	2039	520
2040	525	2040	525
2041	530	2041	530
2042	535	2042	535
2043	540	2043	540
2044	545	2044	545
2045	550	2045	550
2046	555	2046	555
2047	560	2047	560
2048	565	2048	565
2049	570	2049	570
2050	575	2050	575
2051	580	2051	580
2052	585	2052	585
2053	590	2053	590
2054	595	2054	595
2055	600	2055	600
2056	605	2056	605
2057	610	2057	610
2058	615	2058	615
2059	620	2059	620
2060	625	2060	625
2061	630	2061	630
2062	635	2062	635
2063	640	2063	640
2064	645	2064	645
2065	650	2065	650
2066	655	2066	655
2067	660	2067	660
2068	665	2068	665
2069	670	2069	670
2070	675	2070	675
2071	680	2071	680
2072	685	2072	685
2073	690	2073	690
2074	695	2074	695
2075	700	2075	700
2076	705	2076	705
2077	710	2077	710
2078	715	2078	715
2079	720	2079	720
2080	725	2080	725
2081	730	2081	730
2082	735	2082	735
2083	740	2083	740
2084	745	2084	745
2085	750	2085	750
2086	755	2086	755
2087	760	2087	760
2088	765	2088	765
2089	770	2089	770
2090	775	2090	775
2091	780	2091	780
2092	785	2092	785
2093	790	2093	790
2094	795	2094	795
2095	800	2095	800
2096	805	2096	805
2097	810	2097	810
2098	815	2098	815
2099	820	2099	820
2100	825	2100	825

I. INTRODUCTION

A thesis is a long road with many turns. I have always been interested in computers, and particularly at the level where digital meets analog. I have also been interested in robotics. This thesis has been an opportunity to explore these areas in more depth. A circuit for detecting conducting material in the ground, e.g. landmines, had been developed by Goodnight (Goodnight, 1996) and needed to be adapted for use on an autonomous robot. These circumstances lead me to research the landmine issue.

Landmines and unexploded ordnance (UXO) present an almost insurmountable problem. Detection is a tough technological challenge because the ground is a particularly hard place in which to search. It's properties vary by geographic area, time of the day and weather conditions. The object of the hunt is also getting harder to find. Mines are made today with little or no metal. Ordnance removal is a slow, tedious task with severe consequences for failure.

The problem is immense, and getting larger. The UN estimates there are over 110 million land mines laid, with millions more waiting to be used (UN, 1997). It costs only \$5 to deploy scatterable mines and \$200 to \$1,000 per mine and one life per 5000 to remove them. For every mine removed twenty more are laid. At the current clearance rates, and no new mines laid, it will take *4,000 years* to clear all the mines in Afghanistan. (Walker, 1995)

They are indiscriminate and long lasting. Eight hundred deaths a month are attributed to land mines. Last year 40 French farmers were killed from World War II ordnance in their fields. Significant portions of Cambodia are denied civilian use because of mines.

Practical detection of landmines is presently done primarily with manual search techniques. A member of the local population probes the ground with a nonmetallic probe centimeters at a time. When the probe hits a solid object, it is uncovered and identified. The rate of clearance is on the order of square meters per day. It is a slow, tedious and

dangerous operation. It would be faster and safer to substitute a robot and automated detection for the human.

Goodnight's circuit was not suitable for robot use for several reasons. The circuit depended on a manually turned inductor to balance the search coil. Adjustments could not be made by the robot for varying environment conditions. The circuit was also extremely sensitive to stray capacitance. Therefore I modified the Goodnight circuit to take these into account.

This then, is the backdrop from which I began to develop a robot and attempt to find landmines. This thesis will review landmine sensing technologies currently being researched and briefly review possible robot types. Then a description of the circuit eventually decided upon, with its theory of operation, construction details and experimental results.

II. THEORY

A. REVIEW OF SENSING TECHNOLOGIES

The solution to the landmine dilemma has three generally agreed on phases: detection, classification, removal. There is much work in the sensing technology area, which we will cover here. Some of the technologies are suited for ordnance clearance of old battlefields and training areas, others are directed solely at landmine detection. Many of these techniques require significant computer processing, are very large, and require significant electrical power.

No one sensing technology dominates. Solving such a complex problem will probably involve more than one sensing technique, and the fusion of data from many sources.

1. Electromagnetic

a. Magnetic field

(1) Proton Precession Magnetometer. Fluid, usually water, is placed in a container inside a solenoid. The solenoid axis is aligned orthogonally to the field to be measured. The magnetic spin axis of the water's protons are aligned parallel to the solenoid's axis when energized. When the solenoid is instantaneously de-energized, the protons begin to precess about the axis of the magnetic field to be measured. This precession induces an emf in the solenoid proportional to the magnetic field strength. Resolution of 0.1 nT at 10 Hz is possible. (Bartington, 1994)

(2) Optically Pumped Magnetometer. This magnetometer uses the Zeeman effect to measure the ambient field. Circularly polarized light from a cesium metal vapor lamp is directed along the axis of the field to be measured. The light passes through an absorption cell containing cesium metal vapor. The intensity of the beam from the cell is proportional to the magnetic field strength. It has a sensitivity around the 10 pT level. (Healey, 1995)

(3) Flux Gate. Because of its small size, low power requirements and good noise performance, the fluxgate magnetometer is the most versatile magnetic sensor. It converts a static or slowly varying magnetic flux into an alternating voltage which can easily be measured. A core of very high relative magnetic permeability material is surrounded by a solenoid which drives it into saturation. The solenoid current is alternated so as to saturate the core in different directions. When the driving current is removed, a back EMF will be generated in the solenoid. If no external field is present, the EMF will be symmetrical. However, if a field is present, the EMF will be asymmetric, thus containing information about the field. (Jiles, 1991)

For low power, low bandwidth applications a single core configuration would be used, where the driving current and back EMF would be applied from the same coil. Such a configuration has been used for fusing sensors for both land and sea mines. For greater accuracy, two primary coils surrounding cores wound in an opposing sense. Two secondary coils are used, so that the driving signal does not appear in the output. Use of an error feedback signal results in linearity errors as low as 0.001%. (Bartington, 1994)

(4) Hall effect Magnetometer. Hall effect magnetometers use the Hall effect to measure fields down to around a few μT in an area of about a mm^2 .

(5) Magnetoresistors. A relatively new technology involves the variation in resistance in the presence of a magnetic field of certain materials. The magnetoresistive effect is generated by the electron spin orbit coupling. The change in electron distribution changes the scattering of the conduction electrons (Jiles, 1991). Magnetoresistors used in a Wheatstone bridge circuit with two shielded magnetoresistors will produce a voltage that varies as the ambient magnetic field changes. This circuit can be made small and low power, however it detects ferrous materials only. (Healey, 1995)

b. Induction

Induction sensors measure the strength of a secondary magnetic field induced by a primary coil. The resulting field is measured by a secondary coil. Although they only detect conducting material, they are valued for their sensitivity.

c. Electromagnetic Radiation

(1) Ground Penetrating Radar. Ground penetrating radars (GPR) commonly use frequencies of 30 Mhz to 2 Ghz. The strength of the reflected signal depends on target distance, material, and orientation, and the soil characteristics. The returned signal is examined for changes in amplitude, time delay, phase, polarization and propagation direction. GPRs can be placed in four categories: short pulse, video pulse, synthetic pulse, and frequency modulated continuous wave systems. Commercial systems can detect wires and pipes at 13 feet underground. (TR-311, 1993)

(2) Passive Millimeter Detection. Passive millimeter wave sensors (radiometers) detect mines by the difference in reflection of the low level radiation from the sky. Metal and to a lesser extent, plastic, objects appear cold while the surrounding soil is appears hot. Soil moisture has a large effect on sensor performance. Success has been reported, (Yujiri 1996), using a 12 Ghz sensor imaging metal and plastic mines under leaves and sand to a depth of 4 cm. Groot (Groot, 1996) found that surfaced anti-personnel mines and buried anti-tank mines were not visible using a 94 Ghz radiometer.

(3) X-ray Backscatter. Compton Backscatter Imaging (x-ray backscattering) generates an image by detecting the reflected photons from an object. Material with lower electron densities scatter more photons than more electron dense materials do. Since plastics are less electron dense than soil or metal, they can be detected this way, as can steel, which is more electron dense than soil. Since such high frequencies are involved penetration depth is not great, but resolution is good. Generation of x-rays also requires a large power supply and space. (Keshavmurthy, 1996)

2. Miscellaneous

a. Tactile

Vibrations produced by moving a tactile sensor over a surface are different for man made and natural materials. Plastic can be differentiated from metal, rock and wood by the response to a probe inserted in the ground. Many probes can be inserted at once to allow fairly rapid searching. (Arnot, 1996)

b. Odor Sensor

The sensitivity of dogs and certain insects' sense of smell leads hope that the explosives in a mine can be detected. Artificial odor detectors exist but operate at higher concentrations. (Machler, 1995)

c. Ion Mobility Spectrometry

An Ion Mobility Spectrometer detects the presence of a particular molecule by ionizing it and then measuring the time to travel through a magnetic field in a tube. The device is fast and can be compact, but it's sensitivity is not very high. (Machler, 1995)

d. Reversal Electron Attachment

The NO₂ compound in explosives has a high affinity for electrons. Electrons at very low energies that hit the compound form characteristic anions or disassociates in a unique pattern. A detector is being developed that can sense these anions or disassociation patterns. (Chemical and Engineering News, 1997)

e. Nuclear Quadrupole Resonance

Some nuclei, such as nitrogen-14 possess quadrupole moments. When subjected to radio frequency radiation they respond with unique signals depending on the nucleus and it's chemical environment. (Chemical and Engineering News, 1997)

f. Neutron analysis

A target illuminated with both fast and slow neutron beams will emit y-rays of characteristic energies. Y-rays are analyzed from interactions from nuclei reacting with fast and slow neutrons. Identification is based on the combined y-ray information.

(Chemical and Engineering News, 1997)

B. COIL THEORY

1. Magnetic Field and Flux

All current carrying conductors produce a magnetic field. A conductor formed into a coil will produce a magnetic field that can be calculated from the Biot-Savart law:

$$B(x) = \frac{\mu_o i R^2}{2(R^2 + x^2)^{3/2}},$$

where x is the distance on the axis from the coil, R is the coil radius, μ_o is the permeability of free space and i is the current through the coil.

The flux of the magnetic field, Φ_B , is defined as

$$\Phi_B = \int B \cdot ds.$$

A coil with constant current will produce a constant magnetic field and flux.

Faraday discovered that relative motion between a conductor and a magnetic field will generate an electro-motive force (emf) in the conductor. The emf generated is given by:

$$\varepsilon = -\frac{d\Phi_B}{dt}.$$

The minus sign indicates that the induced emf will oppose the change in flux.

If we vary the current in the coil, the magnetic field will vary likewise, and according to Faraday,'s law, an emf will be generated in the coil, opposing the change in current.

2. Inductance

If the current is changed in coil, the emf induced by the changing flux will oppose the current change. Inductance, L , is defined as:

$$L = -\frac{\varepsilon}{di/dt}$$

For a flat packed coil of N turns, the flux set up in each turn is the same for all turns. Thus the emf generated would be:

$$\varepsilon = -n \frac{d\Phi_B}{dt}.$$

Equating the emfs generated gives:

$$-n \frac{d\Phi_B}{dt} = -L \frac{di}{dt},$$

and the inductance of the coil, can be written as the proportionality constant between the current and the flux :

$$n\Phi_B = Li \tag{1}$$

3. Mutual Induction

A changing magnetic field creates an electric field:

$$\nabla \times E = -\frac{\partial B}{\partial t}.$$

If conducting material is within the magnetic field of the coil with varying current, the varying electric field will induce circulating currents, called eddy currents, in the material:

$$J = \sigma E.$$

The eddy currents will circulate in a direction that will oppose the change that produced them, according to Lenz's Law. These eddy currents will generate a magnetic field of their own, and that will oppose the field that created them. This means that the lines of flux through the original coil will be reduced. From equation (1), we see that if the flux is decreased the inductance will be also. We will use this interaction to detect the presence of conducting material.

C. RLC OSCILLATOR THEORY

The relationship between voltage, current and energy storage for a capacitor and inductor is given in Table 1.

Device	Voltage	Current	Energy Storage
Capacitor	$v(t) = \frac{1}{C} \int i(t) dt$	$i(t) = C \frac{dv}{dt}$	$E = \frac{1}{2} C (v(t))^2$
Inductor	$v(t) = -L \frac{di(t)}{dt}$	$i(t) = \frac{1}{L} \int v(t) dt$	$B = \frac{1}{2} L (i(t))^2$

Table 1. Capacitor and inductor characteristics

The energy storage of a capacitor depends on the voltage across it, which can be a function of time. Since a discontinuity in energy as a function of time would require an infinite amount of power, energy, hence voltage, must be a continuous function of time for a capacitor. Similarly, the current through an inductor must be a continuous function of time.

The LC circuit shown in Figure 1 contains two energy storage devices, the capacitor and the inductor. At time $t = 0$, a switch was closed, giving the circuit shown, with the capacitor having an initial voltage V_0 , and $i_0 = 0$.

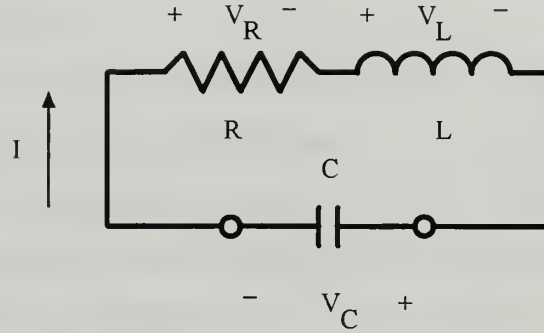


Figure 1. RLC Circuit

With the current direction as shown, and using the relationships in Table 1, the differential equation for the circuit is:

$$L \frac{di(t)}{dt} + Ri(t) + \frac{1}{C} \int i(t) dt = 0.$$

Differentiating once yields:

$$\frac{d^2 i(t)}{dt^2} + \frac{R}{L} \frac{di(t)}{dt} + \frac{1}{LC} i(t) = 0$$

This is a homogeneous differential equation whose solution is of the form $i(t) = Ke^{st}$. The characteristic equation for this RLC series circuit is obtained by substituting the assumed solution into the differential equation and is:

$$s^2 + \left(\frac{R}{L}\right)s + \left(\frac{1}{LC}\right) = 0.$$

The characteristic equation has two roots:

$$s_1 = -\frac{R}{2L} + \sqrt{\frac{R^2}{4L^2} - \frac{1}{LC}},$$

and,

$$s_2 = -\frac{R}{2L} - \sqrt{\frac{R^2}{4L^2} - \frac{1}{LC}}.$$

Depending on the values of R, L, C the roots may be real and equal, $(R^2/4L^2) = (1/LC)$, real and unequal, $(R^2/4L^2) > (1/LC)$, or imaginary and complex conjugates of each other, $(R^2/4L^2) < (1/LC)$. The first two cases are the over damped and critically damped cases and do not concern us.

The imaginary roots can be written as $s_{1,2} = \alpha \pm j\beta$, where $\alpha = (R/2L)$, and $\beta = \sqrt{(1/LC) - (R^2/4L^2)}$. The assumed solution has to be modified for this case to :

$$i(t) = K_1 e^{-(\alpha - j\beta)t} + K_2 e^{-(\alpha + j\beta)t}. \quad (2)$$

Using the initial condition of no current, gives $K_1 + K_2 = 0$. The other initial condition, $di/dt = -(V_0/L)$, is determined by the capacitor initial voltage of V_0

gives $K_1 = -K_2 = -(V_0/2jL\beta)$.

Substituting the constant values in equation 2 and applying Euler's identity gives the current as a function of time:

$$i(t) = -(V_0/L\beta) e^{-\alpha t} \sin t\beta. \quad (3)$$

Using the relationship from Table 1 for the voltage of a capacitor yields:

$$v_c(t) = (V_0/\beta \sqrt{LC}) e^{-\alpha t} \cos[t\beta - \arctan(\alpha/\beta)]. \quad (4)$$

The results, equations 3 and 4, show that the voltage across the capacitor (which is the voltage across the resistor and inductor) is almost 180 degrees out of phase with the circuit current. The oscillations result from the continuous exchange of energy between the capacitor and inductor.

Figure 2 shows the curves for the circuit in Figure 1 with values $R = 2$ ohms, $L = 10$ mH, $C = \mu\text{F}$, and initial capacitor voltage of 10 V.

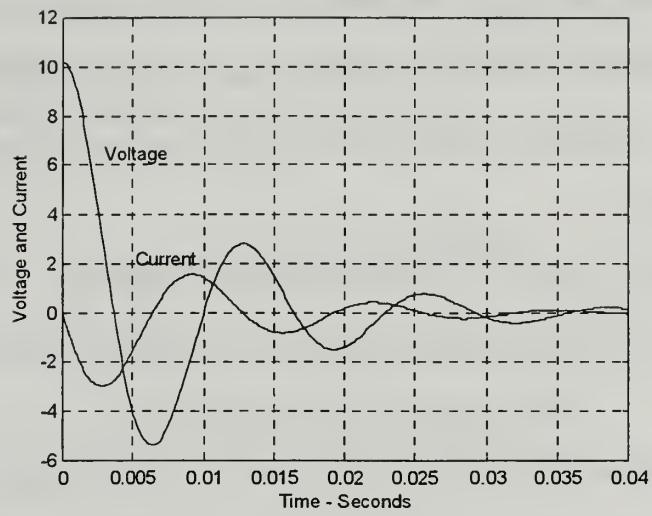


Figure 2. RLC Circuit Response

III. CONSTRUCTION AND OPERATION

A. SENSING CIRCUIT

The circuit developed was based on Anglin, 1977, shown in Figure 3.

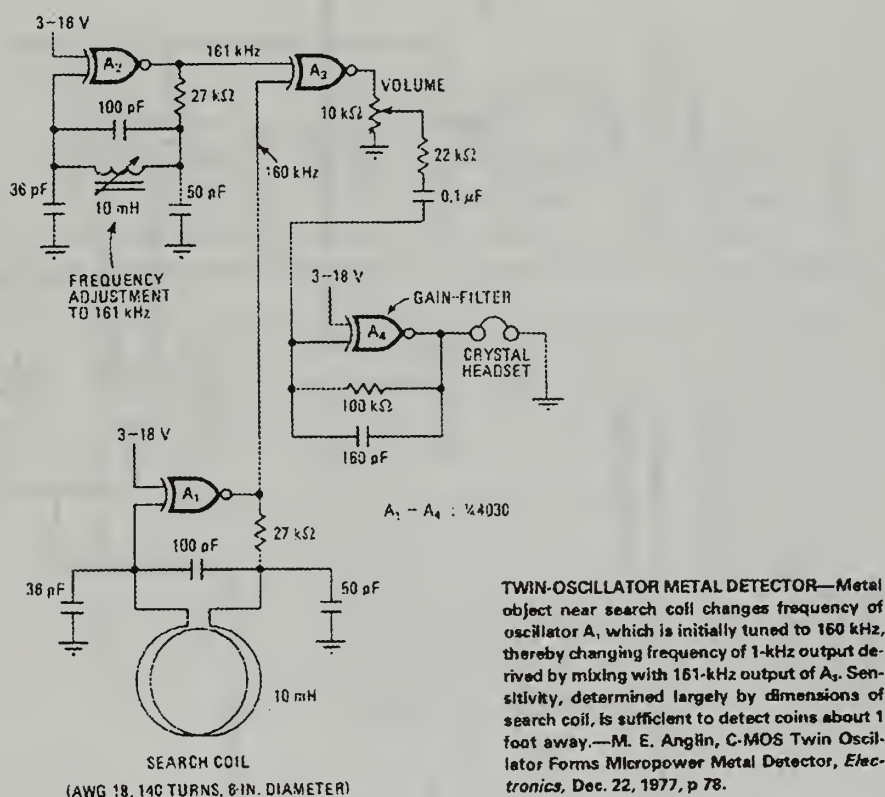


Figure 3. Twin Oscillator Metal Detector

The circuit output of Figure 3 is a tone that varies when conducting material is encountered. The signal from the detecting circuit is mixed with a generated signal that produces a 1 KHz tone. This frequency changes and is detected by an operator on headphones. Since the circuit is to be interfaced to a microprocessor, it's output must be converted to a digital form. The best approach was to count the frequency coming from the sensor circuit directly. The circuit developed is shown in Figure 4. The various parts of the circuit's operation and construction will be explained in the following paragraphs.

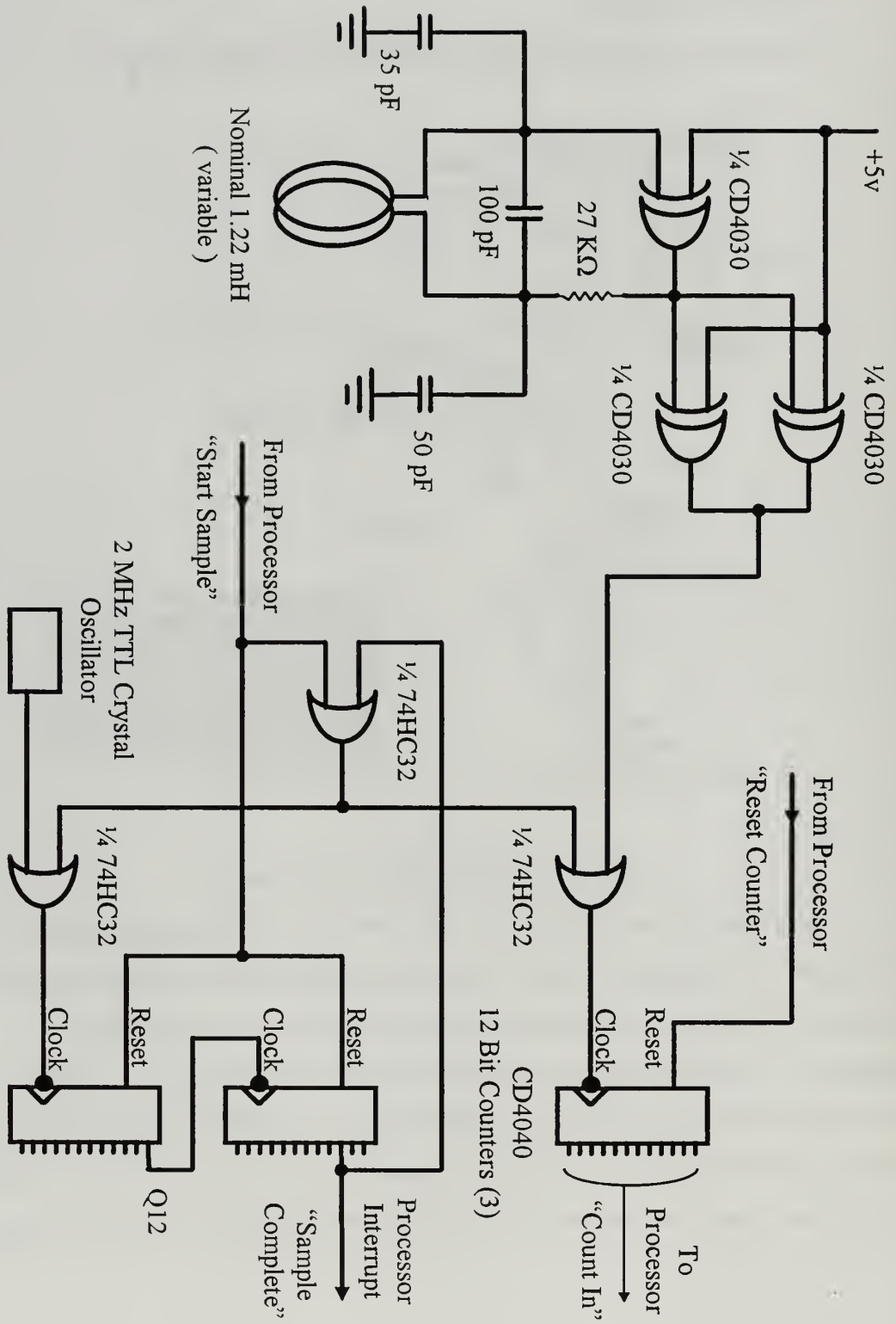


Figure 4. Sensing Circuit Logical Diagram

B. SENSING COIL

Various coils were constructed from thirty gauge wire wound on circular forms. They were of different diameters and number of windings, listed in Table 2, and shown in Figure 5.

Diameter (cm)	Turns	Measured Inductance (mH)	Operating Frequency (KHz)
10	26	.159	1000
15	49	.855	387
20	13	.093	1200
20	25	.342	614
20	34	.633	425
20	49	1.22	280
30.5	70	3.51	169

Table 2. Sensing Coil Measurements

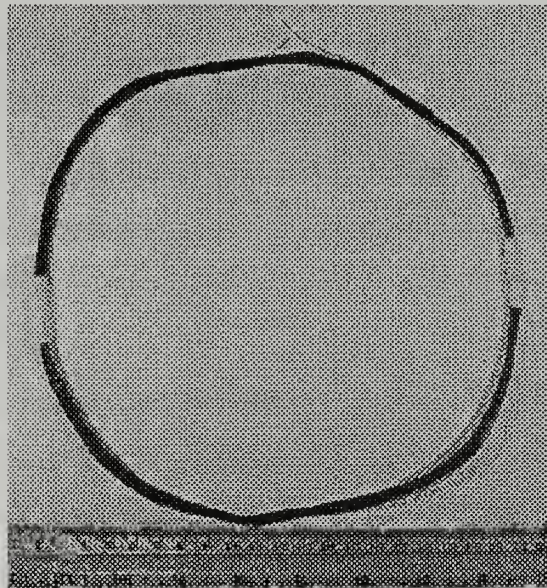


Figure 5. Search Coil

C. OSCILLATOR CIRCUIT CONSTRUCTION

The circuit was initially constructed entirely on a breadboard, with a coaxial cable connecting the coil and the oscillator. While the circuit operated properly, the oscillation frequency was not constant. As will be discussed later, the frequency pulses are counted for a constant period of time. The number of counts varied from sample to sample by up to ten with no conductor present. This noise reduced the sensitivity of the detector to an unacceptable degree. The circuit was also very sensitive to movement, temperature and human presence.

Since the LC circuit uses such a small capacitance (100 pF), it was extremely sensitive to stray capacitance caused by the movement of the coil leads, the movement of wires on the breadboard, and human limbs that happened to be nearby. The oscillator circuit was moved to a small circuit board next to the coil, as can be seen in Figure 6.

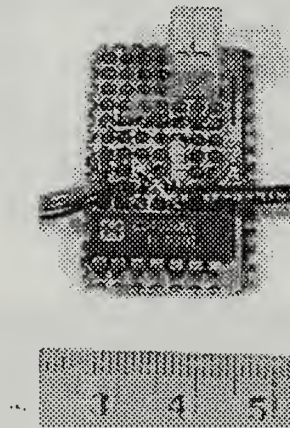


Figure 6. Oscillator Circuit Board

The circuit board was constructed with the components as close together as practicable and on a ground plane. The ground plane removes any stray capacitance influence on the oscillator.

Placing the oscillator as close as possible to the coil had three beneficial effects. The coaxial cable connecting the coil and oscillator, at 200pF per foot intrinsic capacitance, had twice the capacitance as the LC circuit capacitor. Eliminating this capacitance let the circuit oscillate at a much higher frequency with a given coil. The cable capacitance also had a temperature dependence, as seen when warmed just a few

degrees. The circuit operation was more stable since the length of the un-amplified oscillator signal was reduced to the absolute minimum. A coaxial cable was used to connect the amplified oscillator output and the counter circuit, with the outer conductor tied to the ground plane, to prevent the position of the output wire affecting oscillator frequency by stray capacitance.

Capacitors used in the initial construction were of an unknown specification. Operation outside was more variable than inside due to the temperature characteristics of the capacitors. Capacitors of the COG specification were used and operation improved.

Standard CMOS construction techniques were used in constructing the circuit. A small bypass capacitor was placed across the power supply pins of the CD4030 to reduce the power supply line fluctuations caused when the chip suddenly turns on. The unused inputs were grounded to prevent oscillation.

D. OSCILLATOR CIRCUIT OPERATION

Figure 7 shows the oscillator portion of the sensing circuit. The key to the operation of the circuit is the LC tank formed by the capacitor C_3 and inductor L , the search coil. The tank's frequency will change in the presence of conducting material as described before.

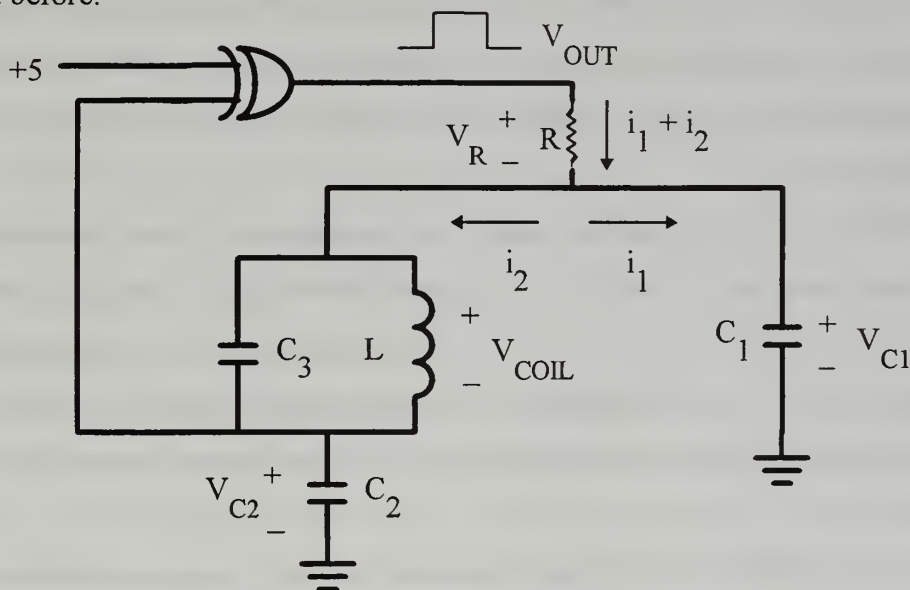


Figure 7. Oscillator Circuit Diagram

The logic gate in Figure 7 is a CD4030 CMOS exclusive OR gate (XOR). Since one input is tied to logic one (+5 Vdc), the output of the gate will be opposite of the other input. A voltage level of 3.155 Vdc or higher on the input is a logic level one, and a logic level zero is 2.45 Vdc or below. When the gate is on, it supplies 5 Vdc through the upper FET in its output stage. See Figure 8.

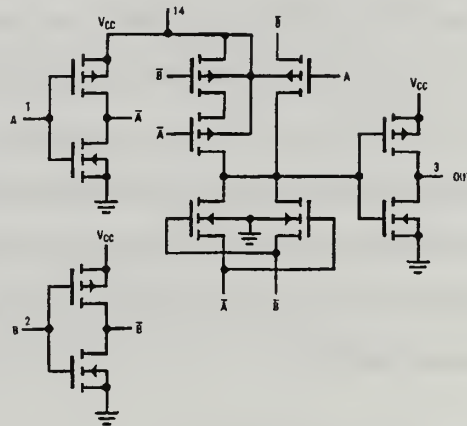


Figure 8. CD4030 Gate Schematic

When the output is logic level zero, it connects the output to ground through the lower FET, and is essentially at ground potential.

The sensing circuit was simulated on MicroSim_8, a circuit simulation program based on PCSPICE. Since the simulation library for the CD4030 chip was not available, circuit simulation was divided into 2 phases. When the XOR gate outputs a logic one, it was replaced with a 5 volt source. When the gate outputs a logic level zero, it was replaced by a ground.

The simulation started with all voltages and currents zero. Since the gate output a logic level one, it was replaced with a 5 volt source. The voltage at the upper terminal of C2 (VC2 in Figure 7) was monitored and the simulation continued until it reached the logic one level, 3.155 Vdc. The voltages of the capacitors and current through the inductor was recorded and entered as initial conditions for the other phase of the simulation.

Since at 3.155 Vdc the XOR gate output will go low, it was replaced with a ground. The initial conditions were entered. The VC2 was monitored until it reached

2.45 Vdc, the logic zero level. The voltages and currents were recorded and used as initial conditions for the other phase.

Circuit voltages were measured with a digital storage oscilloscope at the output and the upper terminals of C1 (VC1) and C2 (VC2). From VC1 and VC2 the voltage across the coil and resistor R of Figure 7 was calculated. The measured waves are plotted in Figures 9, 10, 11 and 12. The results of the SPICE simulation are plotted in Figures 13 and 14. Figure 13 shows the voltages across C1, C2, the coil and the output. Figure 14 plots the currents through the inductor L (the search coil), capacitors C1, C2 and C3, and through R. All currents are positive from the top of a component downward.

As can be seen, the shapes of the simulated waves matches well with those measured. The period of oscillation was faster than actual, and the voltage across the coil larger than measured. However, the wave forms did match well with the measured waves. The value of this simulation was the current waves, which are not easily measured.

When the XOR gate is at logic one, current is coming from the gate through resistor R. The power delivered by the gate makes up for the losses suffered in the oscillator by the circuit resistance. As the gate comes on the voltage across the coil is nearly zero, and current is through the coil and C3 is nearly at it's maximum. Current and voltage are almost 180 degrees out of phase, as seen in the discussion of the RLC circuit previously. The current is going through the coil from bottom to top and the current through C3 is going in the opposite direction. Current is circulating around the tank circuit. Some of the gate current is also charging capacitor C1, while C2 is discharging. As the currents die away, the voltage across the coil becomes a maximum and the currents a minimum. Current in the tank circuit begins circulating in the opposite direction, and C2 begins charging up.

When the voltage on C2 reaches 3.155 Vdc, the gate turns off. This makes no immediate difference to the current circulating in the tank circuit. However, current is now flowing back through resistor R to ground, through the turned off XOR gate. As can be seen from the measured voltages in Figure 9, the output square wave is not a 50% duty cycle, it is on more than it is off.

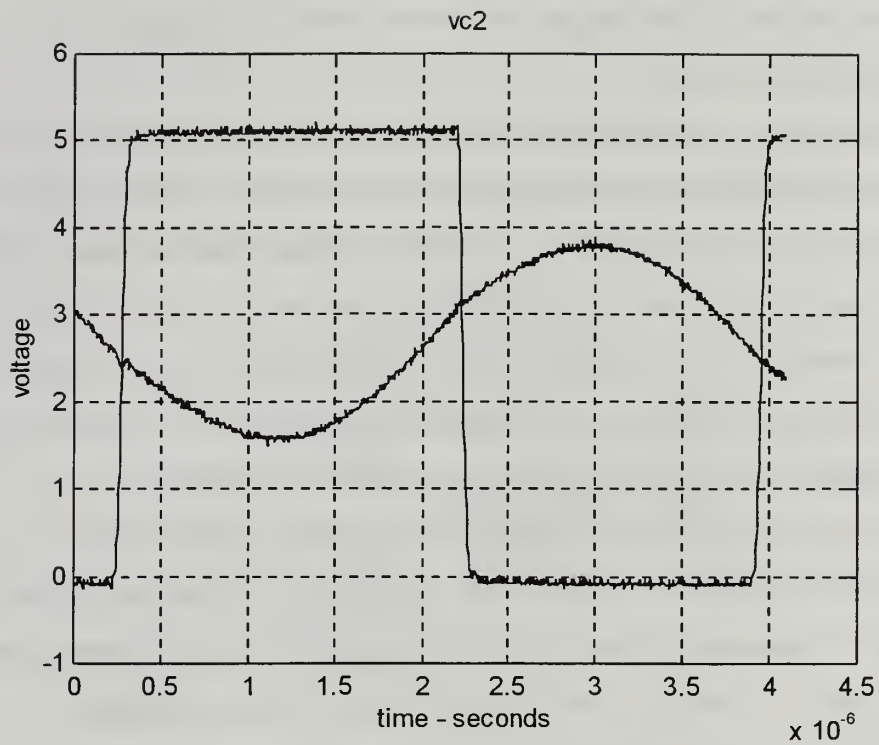


Figure 9. C2 Voltage Vs Output Voltage

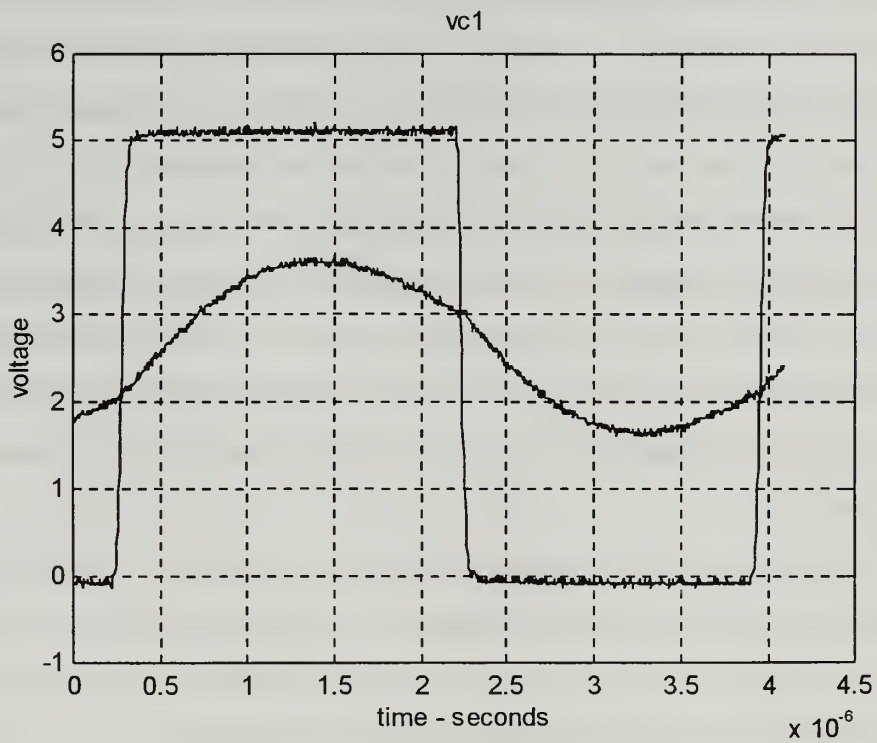


Figure 10. C1 Voltage Vs Output Voltage

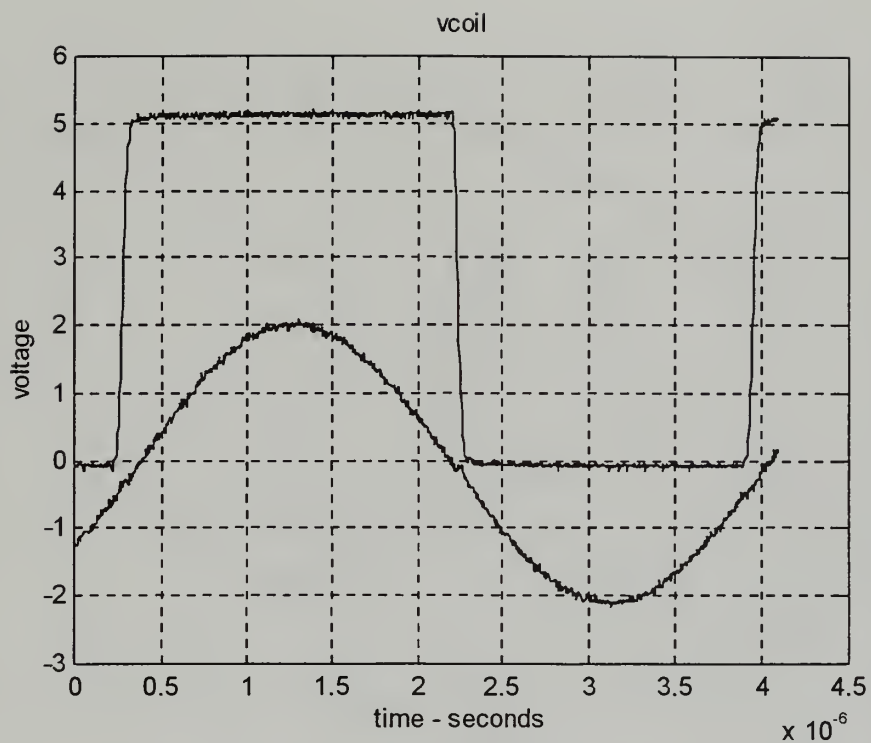


Figure 11. Voltage Across the Coil Vs Output Voltage

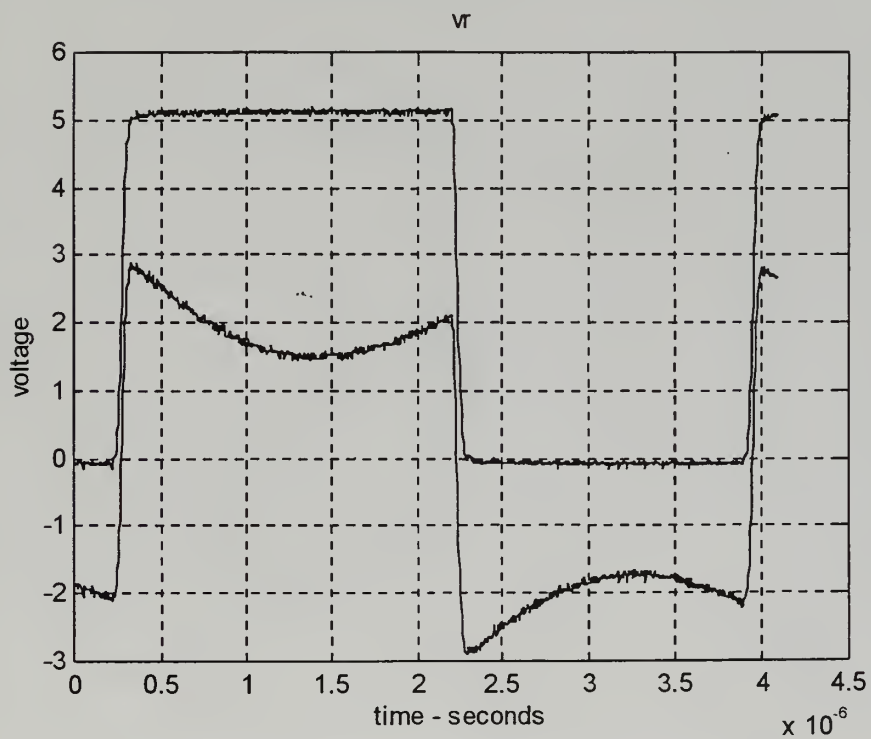


Figure 12. Resistor Voltage Vs Output Voltage

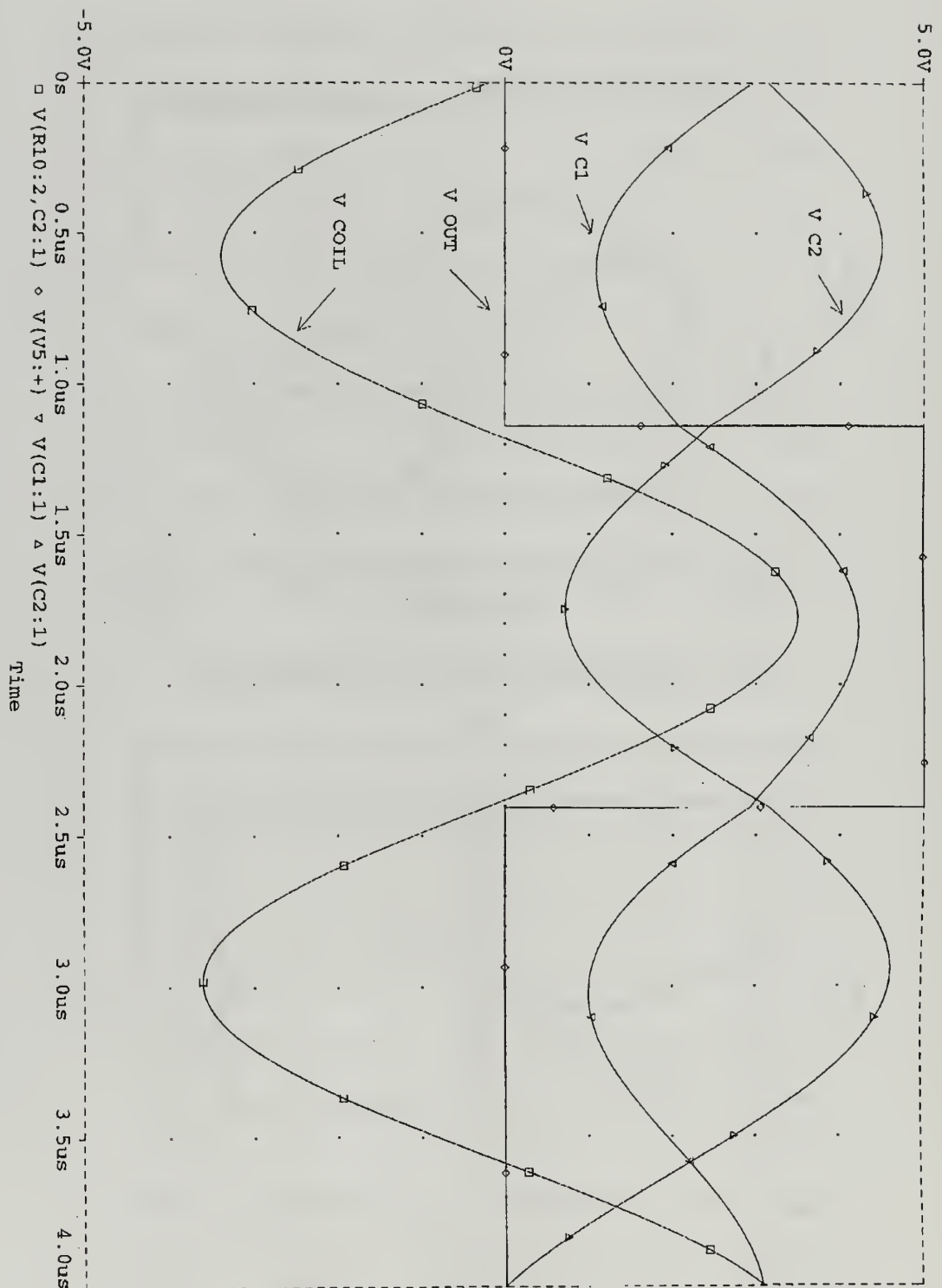


Figure 13. SPICE Simulation Circuit Voltages

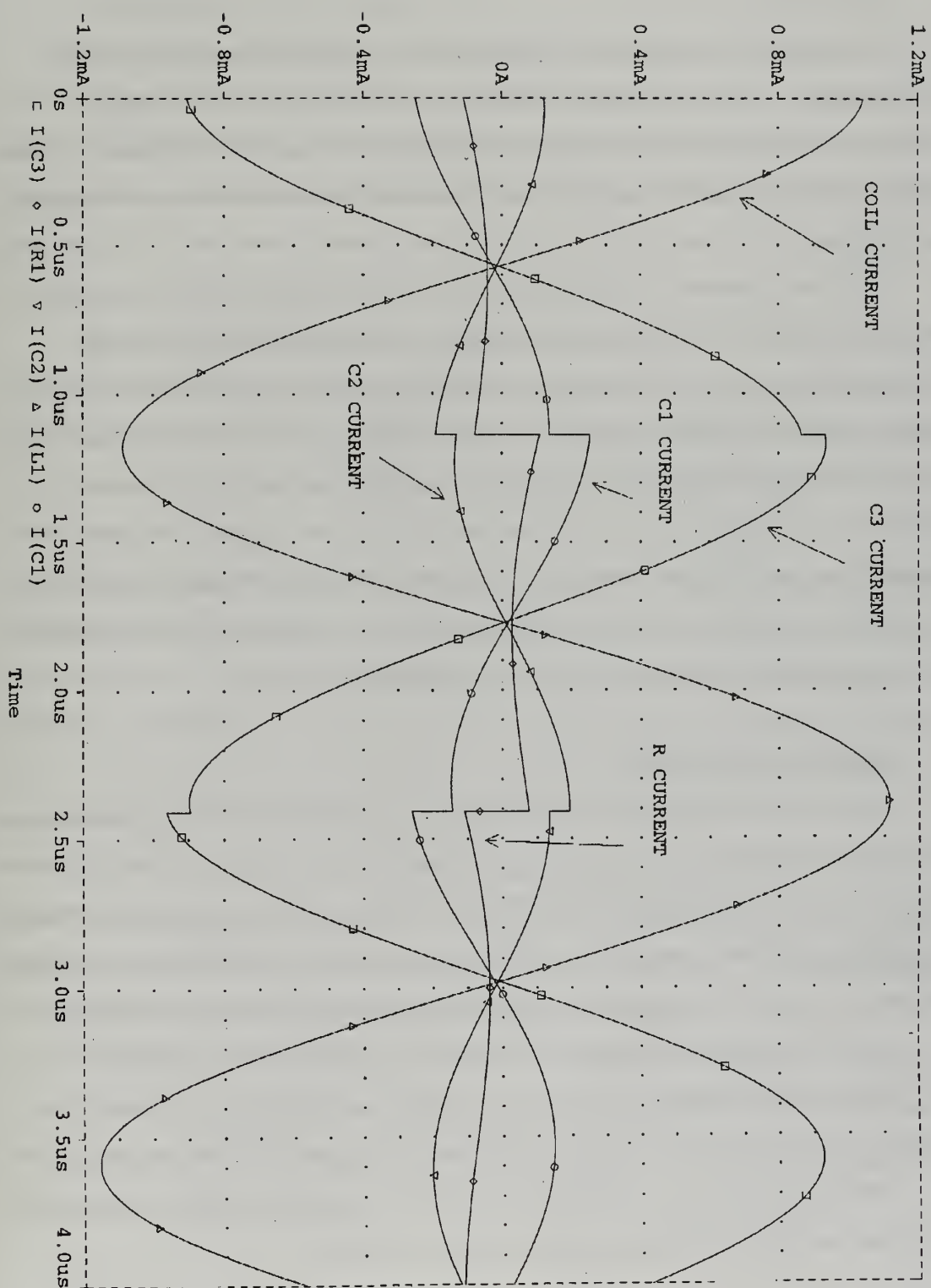


Figure 14. SPICE Simulation Circuit Currents

E. COUNTING CIRCUIT

The output of the coil circuit is monitored by counting the pulses of the square wave it produces. The coil output is counted by a CMOS CD4040 12 bit counter. CMOS was used because of its low power requirements and good noise immunity. Since only the lower 8 bits vary from sample to sample, one counter is sufficient even though it does roll over.

The pulse generator provides the time base for counting pulses from the coil. More important than the exact time of the pulse is consistency from pulse to pulse. Crystal oscillators are very stable and so was used here, and in the TTL package required no further circuitry. CMOS CD4040 12 bit counters were used to divide down the crystal frequency. To get the desired pulse length two counters were cascaded. The most significant bit of the lower counter was the clock for the upper counter. This also facilitated changing the pulse length by simply moving the “Sample Complete” line (Figure 4) to a different counter output. The counting circuit was constructed on a breadboard, which was suitable for initial construction and allowed rapid changes.

F. MICROPROCESSOR

The controller used to direct operations is a Tiny Giant from Z-World Engineering. It uses a Z180 microprocessor running at a clock speed of 9.216 MHz. It has 256K bytes of battery back static RAM and 256K EEPROM. It has two serial ports and 16 general purpose digital I/O lines arranged in two 8 bit ports, PA and PB. The I/O lines can be bit configured for input or output, and the input lines can generate processor interrupts.

The 12 bits of the coil counter are connected to I/O lines PB0 to PB6 and PA0 to PA4. Input bit PB7 generates the processor interrupt, “Count Complete”. Lines PA5 through PA7 are outputs, PA7 “Reset”, PA6 “Start count”, and PA5 indicates mine found.

The Tiny Giant is programmed with Z-World’s Dynamic C compiler, a near ANSI C compliant compiler. Maximum program size is 4,000 lines.

G. SAMPLING CIRCUIT OPERATION

The processor prepares for a sample cycle by asserting the “Start Sample” line high. Bringing “Start Sample” high forces the first OR gate output high, which in turn forces the second level OR gates to go high, blocking the pulse trains of the coil and 2 MHz crystal from their respective counters. The “Start Sample” line high also resets the pulse counters. The “Reset Counter” line is then brought high, then low, clearing the coil counters.

The sample is initiated by de-asserting the “Start Sample” line. This forces the output of the first OR gate low, since the pulse counters have been cleared, and their output is low also. The outputs of the second level OR gates now depend on the coil and crystal outputs. Since these OR gate outputs are the counter clock inputs, the counters begin counting.

The pulse counters count until the output that has the “Sample Complete” line on it goes high. When this happens, the first level OR gate’s output is forced high. This in turn forces the second level OR gates high, blocking the coil and crystal pulse trains, stopping the counters. The “Sample Complete” line going high also interrupts the Tiny Giant. The processor then reads the number of pulses from the coil counter. Refer to lines 102 through 108, in Appendix A for details.

To allow for the variation of coil counts due to noise while no conductors are present, the microprocessor computes a 16 count moving average while the next count is being taken. A detection is signaled if the latest count is greater than 5 above the running average. Refer to lines 82 through 87, in Appendix A for details.

The sensor coil used oscillates in the circuit at 425 KHz. To obtain an adequate number of counts to get reliable detections, a pulse length time of 0.13 seconds was best. It was a trade off between number of counts difference in a pulse and the speed of advance that this would allow the robot.

H. ROBOT

A three wheel configuration using differential drive front wheels with a single passive rear wheel was built. To get sufficient ground clearance, 25 cm diameter tires were fitted. The treads were made of packing foam with a 10 cm tread to minimize footprint pressure. The wheels are driven by two 24 volt DC motors using two 3 amp-hour 12 volt DC batteries. The motors are powered by a SGS-Thomson dual full bridge driver chip controlled by a Technological Arts ADAPT11 68HC11 microprocessor. See Figure 15.

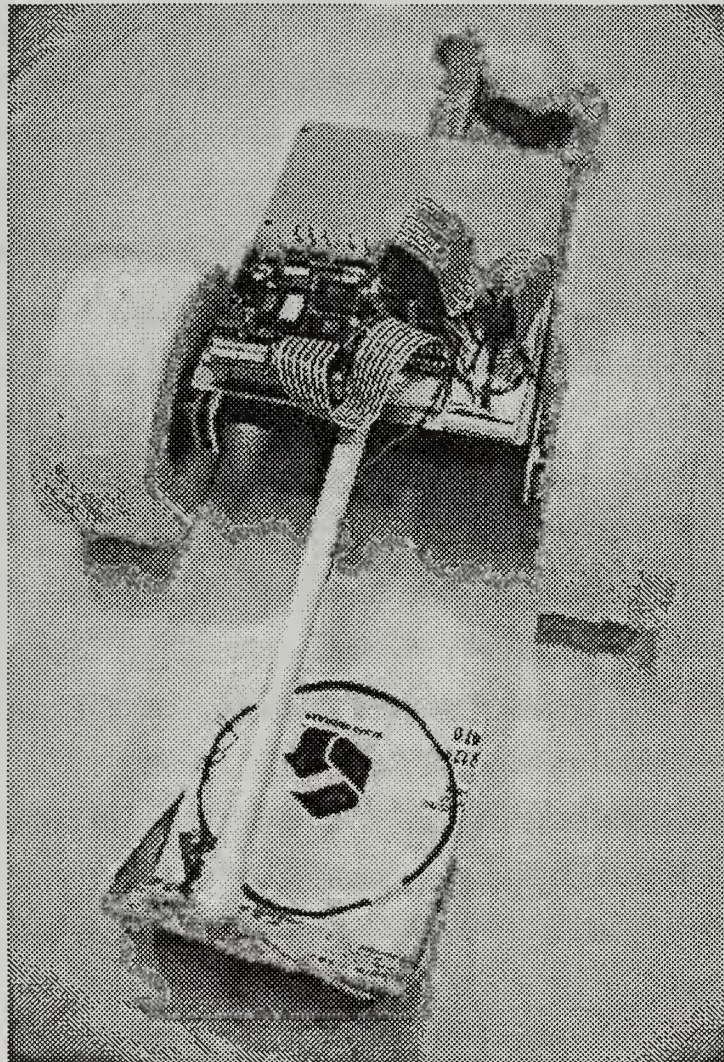


Figure 15. The Robot

Originally, the motors drove the wheels directly. Because the robot has relatively large tires, the motors had to drive at low speeds to allow a reasonable search speed. To drive them at such a slow speed, the width of the driving pulses was very narrow, which caused the motors to operate very roughly. To solve this problem a reduction gear assembly was constructed with a 33 tooth gear on the motor driving a 63 tooth gear on the wheel. Figure 16 shows their construction.

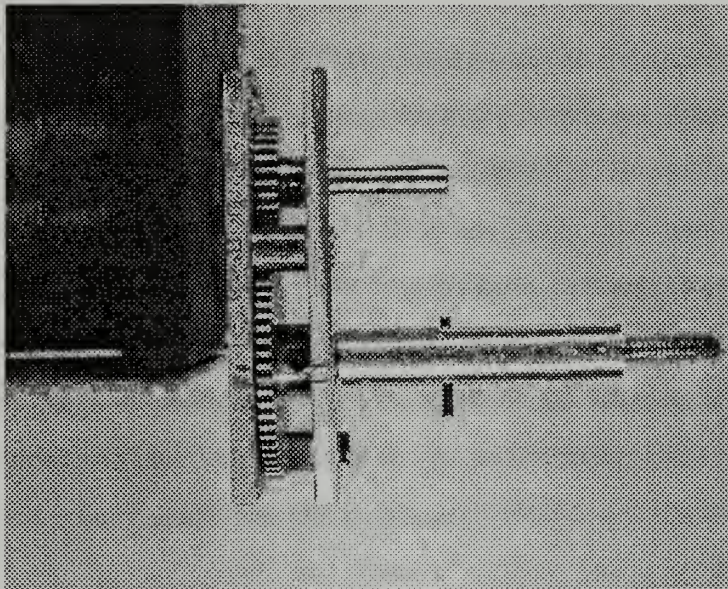


Figure 16. Shaft Reduction Gear Assembly

1. 68HC11

The Motorola 68HC11 is a powerful 8 bit data 16 bit address microcontroller that is attractive for several reasons. Twenty six general purpose I/O lines are available. It can provide two pulse width modulation (PWM) signals in hardware, which are used to control the drive motors. It also has a pulse accumulator register which can count pulses from the motor shaft encoders to keep track of motor movement. An asynchronous serial port is used to communicate with the Tiny Giant which supplies the motor commands. Although not used, it has an 8 channel 8 bit analog to digital converter which could be used to motor drive current.

The ADAPT11 board comes with the 68HC11 and a Xicor X68C75 Microperipheral chip. The X68C75 has 8K EEPROM and two 8 bit I/O port replacement. All bus signals for the 68HC11 and X68C75 are brought out to a 50 pin header.

The 68HC11 is programmed with a near ANSI C compiler from ImageCraft. It supports floating point data types, has a multitasking library, and allows imbedded assembly language programming. Interrupt routines can be written in the C language.

2. 68HC11 / Tiny Giant interface

The Tiny Giant sends motor control commands to the 68HC11 over a asynchronous serial link. The Tiny Giant uses a supplied library function to send the commands, which are the bit masks the 68HC11 will use to control the motor. Commands consist of three ASCII characters, the first indicating the directions of the two motors and the last two indicating the speed of each wheel.

The 68HC11 uses an interrupt routine to handle the incoming characters. When the serial port has received a character an interrupt is raised, and program control is vectored to the routine. Since three characters will be sent, the interrupt routine first disables further interrupts and waits for the next two characters. All three characters are placed in global variables, and a flag is set to let the main program know that a new motor command has been received. The applicable code is on lines 159 through 175 in Appendix B.

3. Pulse Width Modulation

The PWM signals are generated by the 68HC11 hardware after initialization and the loading of the appropriate register with the desired pulse length. The pulses are generated by an internal 68HC11 free running 16 bit clock and three compare registers. The timer counts up to 65,536 (2^{16}) and then rolls over to zero and counts up again. A 68HC11 register, the Output Compare register 1 (OC1), is configured to force two output pins, (PA5 and PA6), high when the free running timer is zero. Output Compare registers OC2 and OC3 are configured to bring PA5 and PA6 low when the counter equals the values in their Timer Output Compare registers TOC2 and TOC3.

The free running timer is driven at one-fourth of the system clock, which 8 MHz. This yields a clock pulse of 0.5 μ sec. The timer will roll over in 65,536 counts of 0.5 μ sec or 32.77 msec, which will be the period for the PWM. The motor orders received from the Tiny Giant are placed in the TOC2 and TOC3 registers and thus control the motor speed.

4. Motor Drive Chip

The SGS-Thomson L298 Dual Full Bridge Driver is a one chip motor drive solution. It allows motor operation in forward and reverse directions from a single polarity power source. Motor direction is controlled by two inputs, Input1 and Input2 of Figure 17. When one input is logic level high and the other low, opposite FETs conduct (1 and 4 or 2 and 3 of figure 17) and the motor spins in one direction. When the input signals are reversed, the opposite FETs conduct and the motor spins in the opposite direction. The Enable input must be high for any of the FETs to conduct, and the PWM signal is applied to here. Motor drive voltage can be as high as 42 volts, and two amps per bridge can be supplied. The logic voltage supply is 5 volts.

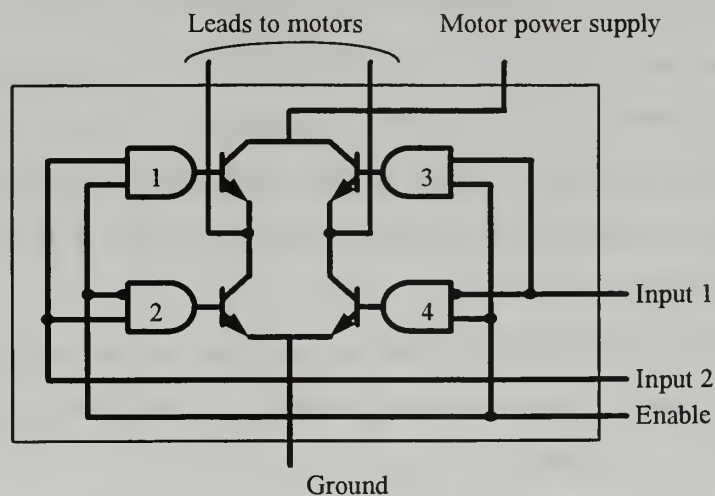


Figure 17. L298 Motor Control Schematic

5. Motors and Shaft Encoders

The motors have an integral reduction gear and shaft encoder. The reduction ratio is 19.7 to 1. The shaft encoder generates two channels of 100 pulses per motor revolution which are offset by 90 degrees allowing a determination of the direction of rotation of the motor shaft. The motor reduction ratio of 19.7:1 and the outer gear box reduction of 1.91:1 gives 3760 pulses per revolution of the robot tires. The tire diameter of 25 centimeters yields approximately 47 pulses per centimeter of robot travel.

6. Wheel / Speed Control

Terrain unevenness and small differences in tire diameter will caused the robot to follow a curved path when a straight one has been ordered. To compensate for this, the pulses from the encoders are periodically compared, and the pulse width of the motor drive changed appropriately.

The 68HC11 has a register associated with one input line, the Pulse Accumulator, that will count the pulses on the input line. One shaft encoder is tied to this input. The other shaft encoder is tied to the clock input of a CD4020 12 bit binary counter. The seventh bit of the counter is connected to an interrupt input of the 68HC11. When the counter sets the seventh bit, the processor is interrupted. The interrupt routine, lines 88 through 107 of Appendix B, reads the Pulse Accumulator and resets it to zero. It then compares that value to the known number of pulses that causes the interrupt. A proportional amount is either added or subtracted from one of the TOC registers to balance the uneven pulses.

This correction is not needed if the robot has been commanded to turn, and the main program will clear the binary counter if it receives a motor command that is not forward or reverse at equal speeds.

IV. TEST RESULTS AND CONCLUSIONS

A. TEST RESULTS

1. Detection Ranges in Air

The detection ranges for different coils was tested in air, with a mine simulant. The simulant is a metal can 5.4 cm in diameter and 7.6 cm tall, which is smaller than the American M-14 antipersonnel mine. The simulant was placed on the coil centerline at various depths, measured to the top of the simulant. Detections were signaled when the counts of a sample period, 0.13 sec, were 5 above a running average of the last 16 sample periods. The range that produced consistent detections was recorded. Table 3 contains the results. The best performing coil, 20/25 could detect an American World War II anti -tank mine, 19 cm diameter 7.6 cm tall, at 28 cm below it's centerline. The 30/70 and 20/13 coils were unstable, periodically signaling false detections.

Coil Diameter (cm) / Turns	Detection Range (cm)
10/26	8.9
15/49	10.5
20/13	14.3
20/25	14.0
20/34	12.4
20/49	11.1
30/70	8.8

Table 3. Detection Ranges

The sensitivity of the 20 cm diameter coils increases with decreasing turns. As the number of turns decreases the frequency of coil oscillation goes up. Since the detection circuit counts the pulses from the circuit, more pulses in a sampling period will give a bigger change in counts in the presence of conducting material. The difference in counts

was recorded when the mine simulant was placed 10.5 cm below the coil on it's centerline for the 20/ 25, 20/34, 20/49 coils, and tabulated in Table 4. As shown the difference in counts varied linearly with oscillation frequency.

Coil Diameter (cm) / Turns	Operating Frequency (KHz)	Freq Change (%)	Count Difference	Count Change (%)
20/49	280	-	8	-
20/34	425	150	12	150
20/25	614	220	16	200

Table 4. Coil Sensitivity

The 20/25 coil was tested for radial sensitivity. The distance from the coil centerline to the center of the simulant at various depths was recorded. Again, the recorded range produced consistent detections. No angular dependence in detection was noted. Figure 18 displays the results. The mine simulant, whose top was just on the surface, could be detected up to 5.1 cm beyond the radius of the coil. This is most likely due to end effects of the coil magnetic field detecting the bottom of the target.

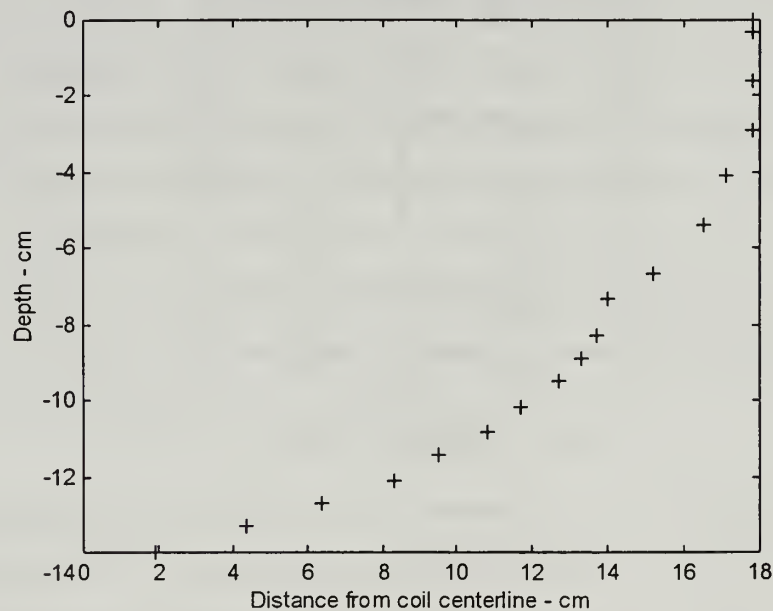


Figure 18. Detection Distance Vs Target Distance From Coil Centerline

2. Robot Performance

Due to an equipment casualty, the robot was not field tested, nor was the integration of the sensor tested.

B. FUTURE WORK

The main area for continued work could be completing the integration of the detector with the robot. Further research could focus on the controlling microprocessor, robot size and capabilities. The efficiency of various search behaviors could be explored. Actions after detection have not be explored.

The Tiny Giant is a large microcontroller board, with many capabilities not needed in the operation of the detection circuit. There are many smaller alternatives, particularly the PicStic© from Circuit Cellar Inc. It has most of the capabilities needed in an area of less than 2.5 cm², requiring much less power.

Much work is being done in smaller wheeled and walking robots. The tradeoffs between computer power, robot capabilities, and power requirements needs to be explored. The usefulness of the swarming behavior of a large number of relatively dumb may be effective in finding mines.

C. CONCLUSION

The adaptation of the sensing circuit has been successful. A 20 cm coil can detect metallic anti-personnel at 14 cm on it's axis and an anti-tank mine at 28 cm. Further investigation into the controlling microprocessor should yield a detector that is small and uses very little power. It should compliment other sensing technologies very well.

APPENDIX A

```
1
2
3 // search.c
4 // revised 14 Sep 97 - 24 Aug 97
5 // Show all counts with running ave.
6
7 #INT_VEC PIOB_VEC INT1
8
9
10
11 int datah, datal;
12 int data__avail;
13
14 main()
15 {
16
17     int i;
18     int index;
19     unsigned int ave;
20     unsigned int total;
21     int counts[16];
22     int ans;
23     int num;
24
25     // PA6,7,5 output, all others input
26     // PA6 Start count, active low
27     // PA7 Reset, active high
28     // PA5 interrupt led
29     output( PIOCA, 0xff );
30     output( PIOCA, 0x1f );
31
32     // All input, PB7 interrupt
33     output( PIOCB, 0xff );
34     output( PIOCB, 0xff );
35     output( PIOCB, PIOB_VEC );
36     output( PIOCB, 0xf7 );
37     output( PIOCB, 0x7f );
38
39     data__avail = 0;
40     index = 0;
41     total = 0;
42     num = 0;
43
44     while ( index < 16 ) {
45         if ( data__avail ) {
46             output( PIODA, 0xc0);           // reset, stop count
47             output( PIODA, 0x40);           // un-reset, stop count
48             output( PIODA, 0x00);           // start count
49             data__avail = 0;
50
51             total += datah;
52             counts[ index ] = datah;
53             index++;
54
55         } // end if
56     } // end while
57
```

```

58     index = 0;
59     ave = total >> 4;
60
61
62     while ( 1 ) {
63
64         if ( data_avail ) {
65
66             if ( datah > ( ave + 5 ) ) {
67                 num++;
68                 printf( "Got it! %x\n", datah );
69                 output( PIODA, 0xc0);      // reset, stop count
70                 output( PIODA, 0x40);      // un-reset, stop count
71                 output( PIODA, 0x00);      // start count
72                 data_avail = 0;
73             }
74             else {
75                 printf( "data %x, ave %x\n", datah, ave );
76                 output( PIODA, 0xc0);      // reset, stop count
77                 output( PIODA, 0x40);      // un-reset, stop count
78                 output( PIODA, 0x00);      // start count
79                 data_avail = 0;
80
81                 total -= counts[ index ];
82                 total += datah;
83                 counts[ index ] = datah;
84                 index++;
85                 index &= 0x0f;
86                 ave = total >> 4;
87             } // end if ( datah > ( ave + 5 ) )
88
89         } // end if ( data_avail )
90     } // end while
91
92
93 } // end main
94
95
96 interrupt reti INT1()
97 {
98
99     EI();
100
101     datal = inport( PIODB );
102     datah = inport( PIODA );
103     datah &= 0x1f;
104     datah <<= 7;
105     datal &= 0x7f;
106     datah |= datal;
107     data_avail = 1;
108     return;
109
110 } // end int
111
112

```

APPENDIX B

```

1
2
3  /*
4  *   base.c
5  *
6  *   Controls the motor operations.  Receives commands from the
7  *   Tiny Giant via the serial port.
8  *
9  *   3 Sep 97
10 *
11 *   Pin connections -
12 *
13 *   Outputs:  pins
14 *
15 *       68HC11 ADAPT11   Colors of plug wires
16 *
17 *       PA5      8       PWM of l motor, 6811 OC3, L298 (EnableB, pin 11)
18 *                      White
19 *       PA6      7       PWM of r motor, 6811 OC2, L298 (EnableA, pin 6)
20 *                      Yellow
21 *       XPB7     42      nc
22 *       XPB6     41      12 volt relay
23 *                      Yellow
24 *       XPB5     40      shaft counter reset
25 *       XPB4     39      24 volt relay
26 *                      Orange
27 *       XPB3     38      right motor direction (L298 Input2, pin 7)
28 *                      Green
29 *       XPB2     37      right motor direction (L298 Input1, pin 5)
30 *                      Blue of blue/green
31 *       XPB1     36      left motor direction  (L298 Input4, pin 12)
32 *                      Red
33 *       XPB0     35      left motor direction  (L298 Input3, pin 10)
34 *                      Blue of blue/red
35 *
36 *       XPA7     14      Debugging info LEDs
37 *       XPA6     15
38 *       XPA5     16
39 *       XPA4     17
40 *       XPA3     18
41 *       XPA2     19
42 *       XPA1     20
43 *       XPA0     21
44 *
45 *   Inputs:
46 *
47 *       PD0      48      Serial in from Tiny Giant
48 *       PA7      6       Shaft encoder input, Pulse Accumulator
49 *       PA0      13      Shaft counter interrupt, IC3
50 *       PA1      12      STOP! interrupt
51 *
52 */
53
54
55 #include <stdio.h>
56 #include <hc11.h>
57 #include <xicor.h>

```

```

58  #include "hcl1_def.h"
59
60  #define SHAFT_INC 128
61  #define SHAFT_TOL 5
62  #define CORR_FACTOR 3
63
64  /* Global data */
65
66  char robot_dir;
67  char l_mtr_spd;
68  char r_mtr_spd;
69  char sci_status;
70  char no_order;
71  int s_travel;
72  int diff;
73  int lspeed, rspeed;
74
75  /*
76  ****
77      shafts()
78
79      Check pulses from both shafts. If not equal, adjust both
80      to maintain equal travel.
81  ****
82  */
83
84  #pragma interrupt_handler shafts
85  void shafts() {
86
87      s_travel = PACNT;
88      PACNT = 0;
89
90      diff = s_travel - SHAFT_INC;
91      if ( diff > SHAFT_TOL ) {
92          lspeed = TOC2;
93          rspeed = TOC3;
94          lspeed += diff << CORR_FACTOR;
95          rspeed -= diff << CORR_FACTOR;
96          TOC2 = lspeed;
97          TOC3 = rspeed;
98      }
99      else if ( diff > -SHAFT_TOL ) {
100          diff = - diff;
101          lspeed = TOC2;
102          rspeed = TOC3;
103          lspeed -= diff << CORR_FACTOR;
104          rspeed += diff << CORR_FACTOR;
105          TOC2 = lspeed;
106          TOC3 = rspeed;
107      }
108
109  } /* end shafts() */
110
111
112
113  /*
114  ****
115      stop()

```

```

116
117     Handle the suicide button, connected to IC2, PA1, pin 12.
118     Will denenergize the 24 volt relay after stopping PWM,
119     wait a little, then denenergize the 12 volt relay, putting
120     itself to sleep forever.
121     Don't bother to clear the interrupt flag, since don't
122     expect to return!
123     ****
124     */
125
126     #pragma interrupt_handler stop
127     void stop() {
128
129         int j;
130
131         OC1M = 0x00;                /* Stop PWM                */
132         for ( j = 0; j < 40000; j++ ) ; /* Wait for things        */
133         XPORTB &= V24_OFF;          /* to settle down         */
134         for ( j = 0; j < 40000; j++ ) ;
135         XPORTB &= V12_OFF;          /* Bye ...                */
136
137     } /* end stop() */
138
139
140
141
142     /*
143     ****
144         order_in()
145
146         Handle SCI input.
147         Designed to get characters that will be sent
148         in threes by the Tiny Giant-
149             1. direction,      robot_dir
150             2. left speed,     l_mtr_spd
151             3. right speed,    r_mtr_spd
152     ****
153     */
154
155     #pragma interrupt_handler order_in
156     void order_in() {
157
158         XPORTA = 0xff;              /* debugging, we're here! */
159         sci_status = SCSR;          /* necessary to clear int flag */
160         robot_dir = SCDR;
161
162         SCCR2 = 0x04;              /* disable interrupt, we'll wait .. */
163
164         while ((SCSR & 0x20) == 0) ; /* check RDRF flag        */
165         l_mtr_spd = SCDR;
166
167         while ((SCSR & 0x20) == 0) ;
168         r_mtr_spd = SCDR;
169
170         SCCR2 = 0x24;              /* OK, interrupt on next command. */
171
172         no_order = 0;              /* let 'em know they got work. */
173

```



```

174     XPORTA = 0;                /* debugging */
175
176 } /* end order_in */
177
178
179
180
181 /*
182 ****
183
184     main()
185
186 ****
187 */
188
189 main() {
190
191     char dummy;
192     int j;
193     int temp;
194
195
196     /* Initialize stuff */
197     no_order = 1;
198     XCR = 0x0c;                /* XPORTA, XPORTB output */
199     XPORTB = V12_ON;
200
201
202     /* setup the suicide switch */
203     TMSK1 = 0x02;             /* IC2 interrupt enabled */
204     TCTL2 = 0x08;             /* IC2 capture falling edge */
205
206
207     /* setup serial comms */
208     BAUD = 0x32;               /* 2400 baud */
209     dummy = SCDR;              /* dummy read to flush rec buffer */
210     SCCR2 = 0x24;              /* enable SCI rx, rx interrupt */
211
212
213     /* setup the L298 */
214     XPORTB |= 0x05;            /* initially forward */
215     XPORTB |= V24_ON;          /* turn 24v relay on before PWM */
216
217
218     /* setup PWM */
219     OC1M = 0x60;               /* enable OC1M5 & OC1M6 */
220     OC1D = 0x60;               /* put 1 on pins PA5 & PA6 */
221     TCTL1 = 0xa0;              /* OC2 & OC3 to zero with successful
222                               /* compare */
223     TOC1 = 0;                  /* when TCNT = 0, OC1 goes high */
224     TOC2 = 0x0001;             /* smallest PWM to start */
225     TOC3 = 0x0001;
226
227     asm( "cli" );              /* enable interrupts */
228
229
230     while ( 1 ) {
231

```

```

232     while ( no_order ) ;          /* wait for the next order    */
233
234     /* got one ...                                */
235     no_order = 1;
236
237     XPORTB |= CTR_RESET;          /* clear shaft counter, no    */
238                                   /* counting, don't want intr */
239
240     TOC2 = 0x01;                  /* zero PWM                    */
241     TOC3 = 0x01;
242
243     dummy = XPORTB;
244     dummy &= 0xf0;                /* clear mtr control bits    */
245     dummy |= robot_dir;          /* set new direction, set by  */
246     XPORTB = dummy;              /* the interrupt routine     */
247
248     temp = l_mtr_spd << 8;
249     TOC3 = temp;
250
251     temp = r_mtr_spd << 8;
252     TOC2 = temp;
253
254     if ( robot_dir == 0x05 && r_mtr_spd == l_mtr_spd ) {
255         XPORTB &= CTR_CNT;        /* want shaft counters      */
256     }
257
258     /* debugging info                                */
259     XPORTA = robot_dir;
260     for ( j = 0; j < 50000; j++ ) ;
261     XPORTA = l_mtr_spd;
262     for ( j = 0; j < 50000; j++ ) ;
263     XPORTA = r_mtr_spd;
264     for ( j = 0; j < 50000; j++ ) ;
265
266 } /* end while(1) */
267
268
269 } /* end main */
270

```


LIST OF REFERENCES

Anglin, Mark, "CMOS Twin Oscillator Forms Micropower Metal Detector", Electronics, 1977.

Arnot, J., Bourdin, R., Hanson, A., Skoczylas, P., "A Mechanical Means of Land Mine Detection Winning Land Mine Detection Project", <http://faramir.mece.ualberta.ca/landmine/winning.html>, 1996.

Chemical and Engineering News, "Searching for better land mine detectors", American Chemical Society, March 10, 1997.

Bartington, G., "Sensors for Low Level, Low Frequency Magnetic Fields", Report for the IEEE Colloquium 'Low Level Low Frequency Magnetic Fields', London, 1994.

Goodnight, C. J., "Design and Evaluation of Mine and UXO Detectors for Autonomous Mobile Robots", Master's Thesis, Naval Postgraduate School, Monterey, 1996.

Groot, J., Dekker, R., van Ewijk, L., "Landmine Detection With an Imaging 94ghz Radiometer" in Detection and Remediation Technologies for Mines and Minelike Targets, Proceedings SPIE 2765, 1996.

Healey, A. J., Webber, W.T., "Sensors for the Detection of Land Based Munitions", NPS-ME-95-003, Naval Postgraduate School, 1995.

Jiles, D., "Introduction to Magnetism and Magnetic Materials", Chapman and Hall, 1991.

Keshavmurthy, E. T., "Analytical Studies of a Backscatter X-ray Imaging Landmine Detection System", in Detection and Remediation Technologies for Mines and Minelike Targets, Proceedings SPIE 2765, 1996.

Machler, P., "Detection Technologies for Anti-Personnel Mines", in Proceedings of the Autonomous Vehicles in Mine Countermeasures Symposium, Monterey, 1995.

Motorola Inc., "M68HC11 E Series Technical Manual", <http://mot-sps.com/books/mcu/m68hc11/lletd.pdf>, 1996.

National Semiconductor, "CD4030M Quad EXCLUSIVE-OR Gate Datasheet", 1988.

SGS-Thomson Microelectronics, "L298 Full Bridge Driver Datasheet", 1995.

Walker, J., "Minerats: Moore's Law in the Minefield", presentation to IEEE Asilomar Microprocessor Workshop, <http://www.fourmilab.ch/minerats/asilomar95.html>, 1995.

Yujiri, L., Fornaca, S., Hauss, B., Shoucri, M., Talmadge, S., "Detection of Metal and Plastic Mines Using Passive Millimeter Waves", in Detection and Remediation Technologies for Mines and Minelike Targets, Proceedings SPIE 2765, 1996.

NAVEODTEHCEN Technical Report TR-311, "Final Report - Technology Assessment for the Detection of Buried Metallic and Non-metallic Cased Ordnance", Naval Explosive Ordnance Disposal Technology Center, 1994.

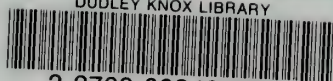
United Nations, <http://www.un.org/Depts/Landmine>, 1997.

INITIAL DISTRIBUTION LIST

1. Defense Technical Information Center 2
8725 John J. Kingman Rd., Ste 0944
Ft. Belvoir, VA 22060-6218
2. Dudley Knox Library 2
Naval Postgraduate School
411 Dyer Rd.
Monterey, CA 93943-5101
3. LCDR Richard Harkins 1
209 Timber Ridge Road
Chesapeake, VA 23320
4. Xiaoping Yun 1
Department of ECE, EC/Yx
Naval Postgraduate School
Monterey, CA 93943-5121
5. LT Jeffrey Schmidt 1
20A S.W. Cutoff
Northboro, MA 01532

DUDLEY KNOX LIBRARY
NAVAL POSTGRADUATE SCHOOL
MONTEREY CA 93943-5101

DUDLEY KNOX LIBRARY



3 2768 00342802 0